A FULLY COMPUTABLE POSTERIORI ERROR ESTIMATE FOR THE STOKES EQUATIONS ON POLYTOPAL MESHES

FENG BAO*, LIN MU†, AND JIN WANG‡

Abstract. In this paper, we present a simple a posteriori error estimate for the weak Galerkin (WG) finite element method for the Stokes equation. This residual type estimator can be applied to general meshes such as polytopal mesh or meshes with hanging nodes. The reliability and efficiency of the estimator are proved in this paper. Four numerical tests demonstrate the effectiveness and flexibility of the adaptive mesh refinement guided by the designed error estimator.

Key words. weak Galerkin, finite element methods, Stokes equations, a posterior error estimate, polytopal meshes

AMS subject classifications. Primary: 65N15, 65N30; Secondary: 35J50

1. Introduction.

The weak Galerkin (WG) method is a natural extension of classical finite element methods for the discontinuous functions. This method was first proposed by Wang and Ye in [49] as a general framework for solving partial differential equations (PDE). The key in WG formulation is to replace the classical derivatives by the weakly defined discrete derivatives. Then by adding a parameter-free stabilizer, one can derive a stable, symmetric, and positive definite formulation. Therefore, the advantages of WG methods include the flexibility of employing polygonal meshes and a natural way to design high-order numerical schemes by using polynomials with higher degrees. WG method has been used to solve different PDEs on general polytopal meshes, such as [28, 29, 30, 31, 32, 50, 51].

In recent studies, many numerical schemes, such as discontinuous Galerkin (DG) methods, hybridized DG (HDG) methods, virtual element, etc, have been developed and analyzed on general polytopal meshes [6, 7, 8, 9, 10, 11, 12, 21, 35, 36, 37, 38, 39, 41, 17, 40]. On the other hand, the a priori error estimate has been investigated for corresponding PDEs. The a posteriori error estimate and adaptive finite element methods have been widely used in modern computational science and engineering to obtain better accuracy with minimum effort for the simulation of singular problems. It can be achieved through adaptive mesh refinement that adds extra resolutions at places of greater importance. However an effective a posteriori error estimator based on polygonal meshes is still challenging to develop [15, 53] due to the technical difficulties in analysis. Most efforts in a posteriori error analysis are still based on simplicial meshes and strong assumptions[13, 14, 16, 22, 25, 34, 46, 47]. In reference [15], the authors designed an polygonal error estimator for the virtual element method. Ref-

*Department of Mathematics, Florida State University, FL, 32306 USA (bao@math.fsu.edu). The author's research is partially supported by Tennessee Center of Excellence in Applied Computational Science and Engineering, National Science Foundation under grant number 1720222, and ORAU Ralph E. Powe Junior Faculty Enhancement Award.

†Computer Science and Mathematics Division Oak Ridge National Laboratory, Oak Ridge, TN, 37831,USA (mul1@ornl.gov). The author's research is based upon work supported in part by the U.S. Department of Energy, Office of Science, Office of Advanced Scientific Computing Research, Applied Mathematics program under award number ERKJE45; and by the Laboratory Directed Research and Development program at the Oak Ridge National Laboratory, which is operated by UT-Battelle, LLC., for the U.S. Department of Energy under Contract DE-AC05-00OR22725.

‡Department of Mathematics, University of Tennessee at Chattanooga, Chattanooga, TN, 37403, USA (jin-wang02@utc.edu). The author acknowledges partial support from NSF grant (number 1520672) and partial support from Tennessee Center of Excellence in Applied Computational Science and Engineering.

erence [24, 26] developed a simple posteriori error estimator for weak Galerkin finite element approximation for Poisson equations. Obviously, the adaptive mesh refinement process will be more effective and local for the polytopal finite element methods that allow general polygon/polyhedron. The Stokes equations describe steady-state fluid flows in the limit of zero Reynolds number, where the inertial acceleration and convection can be dropped from the Navier-Stokes equations. The Stokes model has been used as a canonical example in both mathematical analysis and algorithm development related to fluid motion. In the present study, we use the Stokes problem to demonstrate the application of our adaptive WG formulation and error estimates.

We establish a simple a posteriori error analysis for the weak Galerkin finite element approximation [30] to the Stokes equation. This fully computable error estimator can be applied on general polygonal/polyhedral meshes. Also the error estimate is computed locally on each element T, and thus can be carried out in a parallel fashion. In fact, our a posteriori error estimator only consists of the parameter-free stabilizer and data oscillation. Both of them are computed locally on each element T. Because of such properties as being fully computable, and involving only local and simple calculation, our error estimator is efficient and effective in the adaptive procedure.

For simplicity, we consider a model problem that seeks an unknown function $\mathbf{u}$ satisfying

$$-\Delta \mathbf{u} + \nabla p = \mathbf{f}, \quad \text{in } \Omega, \tag{1.1}$$

$$\nabla \cdot \mathbf{u} = 0, \quad \text{in } \Omega \tag{1.2}$$

$$\mathbf{u} = 0, \quad \text{on } \partial\Omega, \tag{1.3}$$

where Ω is a polytopal domain in $\mathbb{R}^d$ (polygonal or polyhedral domain for $d = 2, 3$).

For a bounded domain D in $\mathbb{R}^d$, we denote by $H^s(D)$ the standard Sobolev space of functions with regularity $s \geq 0$, with norm $\|\cdot\|_{s,D}$ accordingly. For $s = 0$, we write $L^2(D)$ instead of $H^0(D)$ and use norm $\|\cdot\|_D$. When $D = \Omega$, we denote $\|\cdot\|_s := \|\cdot\|_{s,\Omega}$ and $\|\cdot\| := \|\cdot\|_{0,\Omega}$. Furthermore, we introduce the space $H(\mathrm{div}; \Omega) := \{\mathbf{v} \in L^2(\Omega)^d : \nabla \cdot \mathbf{v} \in L^2(\Omega)^d\}$ with the norm $\|\mathbf{w}\|^2_{H(\mathrm{div},T)} := \|\mathbf{w}\|^2 + \|\nabla \cdot \mathbf{w}\|^2$, which will be used later. Finally, the standard inner product $(\cdot, \cdot)$ for $L^2(\Omega)^d$ will also be used.

The weak form in the primary velocity-pressure formulation for the Stokes problem (1.1)-(1.3) seeks $\mathbf{u} \in [H^1(\Omega)]^d$ and $p \in L^2_0(\Omega)$ satisfying $\mathbf{u} = 0$ on $\partial\Omega$ and

$$(\nabla \mathbf{u}, \nabla \mathbf{v}) - (\nabla \cdot \mathbf{v}, p) = (\mathbf{f}, \mathbf{v}), \tag{1.4}$$

$$(\nabla \cdot \mathbf{u}, q) = 0, \tag{1.5}$$

for all $\mathbf{v} \in [H^1_0(\Omega)]^d$ and $q \in L^2_0(\Omega)$. Here, $L^2_0(\Omega) := \{q \in L^2(\Omega),\ \int_\Omega q = 0\}$.

The remainder of this paper is organized as follows. Section 2 introduces the construction of the finite element space. In Section 3, we discuss the a priori error analysis results of H^1-error for velocity and L^2-error for pressure respectively. Section 4 is contributed to the a posteriori error estimate. Extensive numerical experiments are carried out in Section 5 to validate the algorithm and theoretical conclusions. The paper concludes with a summary of main results and brief discussion of future research plans, which are presented in Section 6.

2. Weak Galerkin Finite Element Schemes. Let $\mathcal{T}_h$ be a partition of the domain Ω consisting of polygons in two dimensions or polyhedra in three dimensions satisfying a set of conditions specified in [27, 50]. All the elements of $\mathcal{T}_h$ are assumed to be closed and simply connected polygons or polyhedra. We need some shape

regularity for the partition $\mathcal{T}_h$ described as Section 4.1 in reference [27]. Denote by $\mathcal{E}_h$ the set of all edges or flat faces in $\mathcal{T}_h$, and let $\mathcal{E}_h^0 = \mathcal{E}_h \backslash \partial\Omega$ be the set of all interior edges or flat faces. For every element $T \in \mathcal{T}_h$, we denote by h_T its diameter and mesh size $h = \max_{T\in\mathcal{T}_h} h_T$ for $\mathcal{T}_h$.

For a given integer $k \geq 1$, let V_h be the weak Galerkin finite element space associated with $\mathcal{T}_h$ defined as follows

$$V_h = \{\mathbf{v} = \{\mathbf{v}_0, \mathbf{v}_b\} : \ \mathbf{v}_0|_T \in [P_k(T)]^d, \ \mathbf{v}_b|_e \in [P_k(e)]^d, \ T \in \mathcal{T}_h, \ e \subset \mathcal{E}_h\}$$

and

$$V_h^0 = \{\mathbf{v} : \ \mathbf{v} \in V_h, \ \mathbf{v}_b = 0 \text{ on } \partial\Omega\}.$$

We would like to emphasize that any function $\mathbf{v} \in V_h$ has a single value $\mathbf{v}_b$ on each edge $e \in \mathcal{E}_h$.

For the pressure variable, we have the following finite element space

$$W_h = \{q : q \in L_0^2(\Omega), \ q|_T \in P_{k-1}(T)\}.$$

DEFINITION 2.1. *For any $\mathbf{v} = \{\mathbf{v}_0, \mathbf{v}_b\}$, a weak gradient $\nabla_w \mathbf{v} \in [P_{k-1}(T)]^{d\times d}$ is defined on T as the unique polynomial satisfying*

$$(\nabla_w \mathbf{v}, \tau)_T = -(\mathbf{v}_0, \ \nabla \cdot \tau)_T + \langle \mathbf{v}_b, \ \tau \cdot \mathbf{n}\rangle_{\partial T}, \qquad \forall \tau \in [P_{k-1}(T)]^{d\times d}. \tag{2.1}$$

DEFINITION 2.2. *For any $\mathbf{v} = \{\mathbf{v}_0, \mathbf{v}_b\}$, a weak divergence $\nabla_w \cdot \mathbf{v} \in P_{k-1}(T)$ is defined on T as the unique polynomial satisfying*

$$(\nabla_w \cdot \mathbf{v}, \tau)_T = -(\mathbf{v}_0, \ \nabla\tau)_T + \langle \mathbf{v}_b \cdot \mathbf{n}, \ \tau\rangle_{\partial T}, \qquad \forall \tau \in P_{k-1}(T). \tag{2.2}$$

The usual L^2 inner product can be written locally on each element as follows,

$$(\nabla_w \mathbf{v}, \nabla_w \mathbf{w}) = \sum_{T\in\mathcal{T}_h} (\nabla_w \mathbf{v}, \nabla_w \mathbf{w})_T,$$
$$(\nabla_w \cdot \mathbf{v}, q) = \sum_{T\in\mathcal{T}_h} (\nabla_w \cdot \mathbf{v}, q)_T.$$

Now we introduce some bilinear forms on V_h as follows:

$$s_T(\mathbf{v}, \mathbf{w}) = h_T^{-1} \langle \mathbf{v}_0 - \mathbf{v}_b, \mathbf{w}_0 - \mathbf{w}_b\rangle_{\partial T},$$
$$s(\mathbf{v}, \mathbf{w}) = \sum_{T\in\mathcal{T}_h} s_T(\mathbf{v}, \mathbf{w}),$$
$$a(\mathbf{v}, \mathbf{w}) = (\nabla_w \mathbf{v}, \nabla_w \mathbf{w}) + s(\mathbf{v}, \mathbf{w}),$$
$$b(\mathbf{v}, q) = (\nabla_w \cdot \mathbf{v}, q).$$

Denote by Q_0 the L^2 projection operator from $[L^2(T)]^d$ onto $[P_k(T)]^d$. For each edge/face $e \in \mathcal{E}_h$, denote by Q_b the L^2 projection from $[L^2(e)]^d$ onto $[P_k(e)]^d$. We shall combine Q_0 with Q_b by writting $Q_h = \{Q_0, Q_b\}$. Let $\mathbb{Q}_h$ be the L^2 projection from $L^2(T)$ onto $P_{k-1}(T)$.

WEAK GALERKIN ALGORITHM 1. *A numerical approximation for (1.1)-(1.3) can be obtained by finding $\mathbf{u}_h \in V_h^0$ and $p_h \in W_h$ satisfying the following equations:*

$$a(\mathbf{u}_h, \mathbf{v}) - b(\mathbf{v}, p_h) = (\mathbf{f}, \mathbf{v}_0), \quad \forall \ \mathbf{v} \in V_h^0, \tag{2.3}$$
$$b(\mathbf{u}_h, q) = 0, \qquad \forall \ q \in W_h. \tag{2.4}$$

3. Solvability and A Priori Error Estimate. In this section, we shall cite some theoretical conclusions. Define a discrete H^1 equivalent norm,

$$|||\mathbf{v}|||^2 = (\nabla_w \mathbf{v}, \nabla_w \mathbf{v}) + s(\mathbf{v}, \mathbf{v}). \tag{3.1}$$

The boundedness and a certain coercivity for the bilinear form $a(\cdot,\cdot)$ and the boundedness and inf-sup condition for the bilinear form $b(\cdot,\cdot)$ have been proved in the reference ([51]). Thus, the solvability holds true for the weak Galerkin finite element scheme (2.3)-(2.4).

LEMMA 3.1. *The weak Galerkin finite element scheme (2.3)-(2.4) has one and only one solution.*

The following lemma can be found in [51].

LEMMA 3.2. *Assume the exact solution to problem (1.1)-(1.3) has the regularity* $(\mathbf{u}; p) \in [H_0^1(\Omega) \cap H^{k+1}(\Omega)]^d \times (L_0^2(\Omega) \cap H^k(\Omega))$ *with* $k \geq 1$. *Let* $\mathbf{u}_h \in V_h^0$, $p_h \in W_h$ *be the weak Galerkin finite element solution of the problem (2.3)-(2.4). Then, there exists a constant* C *such that*

$$|||Q_h\mathbf{u} - \mathbf{u}_h||| + \|\mathbb{Q}_h p - p_h\| \leq Ch^k(\|\mathbf{u}\|_{k+1} + \|p\|_k). \tag{3.2}$$

Besides, we define the following notation, for $\mathbf{v} \in [H_0^1(\Omega)]^d$, $\mathbf{v}_h \in V_h^0$,

$$\|\mathbf{v} - \mathbf{v}_h\|_{1,h}^2 = (\nabla\mathbf{v} - \nabla_w\mathbf{v}_h, \nabla\mathbf{v} - \nabla_w\mathbf{v}_h) + s(\mathbf{v}_h, \mathbf{v}_h). \tag{3.3}$$

In addition, let $\mathbf{Q}_h$ be the local L^2 projection onto $[P_{k-1}(T)]^{d\times d}$, we have the following properties.

LEMMA 3.3. *On each element* $T \in \mathcal{T}_h$, *we have the following commutative property for* $v \in [H^1(T)]^d$,

$$\nabla_w(Q_h\mathbf{v}) = \mathbf{Q}_h(\nabla\mathbf{v}), \tag{3.4}$$

$$\nabla_w \cdot (Q_h\mathbf{v}) = \mathbb{Q}_h(\nabla\cdot\mathbf{v}). \tag{3.5}$$

The projection property of Q_b and Cauchy-Schwartz inequality give

$$\begin{aligned}\sum_{T\in\mathcal{T}_h}\|Q_0\mathbf{u} - Q_b\mathbf{u}\|_{\partial T}^2 &= \sum_{T\in\mathcal{T}_h}\langle Q_0\mathbf{u} - Q_b\mathbf{u}, Q_0\mathbf{u} - Q_b\mathbf{u}\rangle_{\partial T} = \sum_{T\in\mathcal{T}_h}\langle Q_0\mathbf{u} - \mathbf{u}, Q_0\mathbf{u} - Q_b\mathbf{u}\rangle_{\partial T}\\ &\leq \Big(\sum_{T\in\mathcal{T}_h}\|Q_0\mathbf{u} - \mathbf{u}\|_{\partial T}^2\Big)^{1/2}\Big(\sum_{T\in\mathcal{T}_h}\|Q_0\mathbf{u} - Q_b\mathbf{u}\|_{\partial T}^2\Big)^{1/2},\end{aligned}$$

and hence together with trace inequality, one can obtain

$$\begin{aligned}s(Q_h\mathbf{u}, Q_h\mathbf{u}) &= \sum_{T\in\mathcal{T}_h} h^{-1}\|Q_0\mathbf{u} - Q_b\mathbf{u}\|_{\partial T}^2 \leq \sum_{T\in\mathcal{T}_h} h^{-1}\|Q_0\mathbf{u} - \mathbf{u}\|_{\partial T}^2\\ &\leq Ch^{2k}\|\mathbf{u}\|_{k+1}^2.\end{aligned}$$

Thus by the triangular inequality, the above lemma, inequality, and the projection property of $\mathbf{Q}_h$, one has

$$\begin{aligned}\|\mathbf{u} - \mathbf{u}_h\|_{1,h}^2 &\leq \|\mathbf{u} - Q_h\mathbf{u}\|_{1,h}^2 + |||Q_h\mathbf{u} - \mathbf{u}_h|||^2\\ &= \|\nabla\mathbf{u} - \nabla_w Q_h\mathbf{u}\|^2 + s(Q_h\mathbf{u}, Q_h\mathbf{u}) + |||Q_h\mathbf{u} - \mathbf{u}_h|||^2\\ &= \|\nabla\mathbf{u} - \mathbf{Q_h}(\nabla\mathbf{u})\|^2 + s(Q_h\mathbf{u}, Q_h\mathbf{u}) + |||Q_h\mathbf{u} - \mathbf{u}_h|||^2\\ &\leq Ch^{2k}\big(\|\mathbf{u}\|_{k+1}^2 + \|p\|_k^2\big).\end{aligned}$$

Moreover, the triangular inequality and the projection $\mathbb{Q}_h$ give the following estimate

$$\|p - p_h\| \leq \|p - \mathbb{Q}_h p\| + \|\mathbb{Q}_h p - p_h\| \leq Ch^k\big(\|\mathbf{u}\|_{k+1} + \|p\|_k\big).$$

Thus, we have the following theorem.

THEOREM 3.4. *Assume the exact solution to problem (1.1)-(1.3) has the regularity* $(\mathbf{u}; p) \in [H_0^1(\Omega) \cap H^{k+1}(\Omega)]^d \times (L_0^2(\Omega) \cap H^k(\Omega))$ *with* $k \geq 1$. *Let* $\mathbf{u}_h \in V_h$ *be the weak Galerkin finite element solution of the problem (2.3)-(2.4). Then, there exists a constant* C *independent of* h *such that*

$$\|\mathbf{u} - \mathbf{u}_h\|_{1,h} + \|p - p_h\| \leq Ch^k(\|\mathbf{u}\|_{k+1} + \|p\|_k). \tag{3.6}$$

4. A Posteriori error estimator for the WG method. For simplicity of notation, results shall be presented in two dimensions and the results can be extended to three dimensional problem. First, define a differential operator for a vector function $\mathbf{v} = (v_1, v_2) \in \mathbb{R}^2$ as follows:

$$\mathbf{curl}\ \mathbf{v} = \begin{pmatrix} -\frac{\partial v_1}{\partial y} & -\frac{\partial v_1}{\partial x} \\ -\frac{\partial v_2}{\partial y} & -\frac{\partial v_2}{\partial x} \end{pmatrix}$$

Let $\mathbf{f}_h$ be the L^2 projection of $\mathbf{f}$ to V_h. Then we introduce a local estimator as follows

$$\eta_T^2 = s_T(\mathbf{u}_h, \mathbf{u}_h) + \mathrm{osc}^2(\mathbf{f}, T), \tag{4.1}$$

where $\mathrm{osc}(\mathbf{f}, T)$ is a high order local data oscillation defined by

$$\mathrm{osc}^2(\mathbf{f}, T) = h_T^2 \|\mathbf{f} - \mathbf{f}_h\|_T^2.$$

Define a global error estimator and data oscillation as

$$\eta^2 = \sum_{T \in \mathcal{T}_h} \eta_T^2, \tag{4.2}$$

$$\mathrm{osc}(\mathbf{f}, \mathcal{T}_h)^2 = \sum_{T \in \mathcal{T}_h} \mathrm{osc}(\mathbf{f}, T)^2. \tag{4.3}$$

Let K be an element with e as an edge. It is well known that there exists a constant C such that for any function $g \in H^1(K)$

$$\|g\|_e^2 \leq C\left(h_K^{-1}\|g\|_K^2 + h_K\|\nabla g\|_K^2\right). \tag{4.4}$$

LEMMA 4.1. *Let* $\mathbf{u} \in H_0^1(\Omega)$ *and* $\mathbf{u}_h \in V_h^0$ *be the solutions of (1.1)-(1.3) and weak Galerkin scheme (2.3)-(2.4), respectively. Then there exists a positive constant* C *such that:*

$$\|\mathbf{u} - \mathbf{u}_h\|_{1,h}^2 \leq C\eta^2, \tag{4.5}$$

where $\|\mathbf{u} - \mathbf{u}_h\|_{1,h}^2 = \sum_T \|\nabla \mathbf{u} - \nabla_w \mathbf{u}_h\|_T^2 + h^{-1}\|\mathbf{u}_0 - \mathbf{u}_b\|_{\partial T}^2$.

Proof. We shall apply Helmholtz decomposition first. It is well known [19] that for $\nabla\mathbf{u} - \nabla_w\mathbf{u}_h \in [L^2(\Omega)]^2$, there exist $\mathbf{r} \in H_0^1(\Omega)^2$ (divergence free) and $q \in L_0^2(\Omega)$ $\mathbf{s} \in H^1(\Omega)^2$ such that

$$\nabla\mathbf{u} - \nabla_w\mathbf{u}_h = \nabla\mathbf{r} + \mathbf{curl}\ \mathbf{s} + q\mathrm{I} \tag{4.6}$$

and that

$$\|\mathbf{r}\|_1 + \|\mathbf{s}\|_1 \leq \|\nabla\mathbf{u} - \nabla_w\mathbf{u}_h\|. \tag{4.7}$$

It follows

$$(\nabla\mathbf{u} - \nabla_w\mathbf{u}_h, \nabla\mathbf{u} - \nabla_w\mathbf{u}_h) = (\nabla\mathbf{u} - \nabla_w\mathbf{u}_h, \nabla\mathbf{r} + \mathbf{curl}\ \mathbf{s} + q\mathrm{I}).$$

From the weak form (1.4), we have

$$\begin{aligned}
(\nabla\mathbf{u} - \nabla_w\mathbf{u}_h, \nabla\mathbf{r}) &= (\nabla\mathbf{u}, \nabla\mathbf{r}) - (\nabla_w\mathbf{u}_h, \nabla\mathbf{r}) = (\mathbf{f}, \mathbf{r}) + (\nabla\cdot\mathbf{r}, p) - (\nabla_w\mathbf{u}_h, \nabla\mathbf{r}) \\
&= (\mathbf{f}, \mathbf{r}) - (\nabla_w\mathbf{u}_h, \nabla_w Q_h\mathbf{r}) \\
&= (\mathbf{f}, \mathbf{r} - Q_0\mathbf{r}_0) + \sum_{T\in\mathcal{T}_h} h^{-1}\langle\mathbf{u}_0 - \mathbf{u}_b, Q_0\mathbf{r} - Q_b\mathbf{r}\rangle_{\partial T} - (\nabla_w\cdot Q_h\mathbf{r}, p_h) \\
&= (\mathbf{f} - \mathbf{f}_h, \mathbf{r} - Q_0\mathbf{r}_0) + \sum_{T\in\mathcal{T}_h} h^{-1}\langle\mathbf{u}_0 - \mathbf{u}_b, Q_0\mathbf{r} - Q_b\mathbf{r}\rangle_{\partial T} - (\mathbb{Q}_h(\nabla\cdot\mathbf{r}), p_h) \\
&= (\mathbf{f} - \mathbf{f}_h, \mathbf{r} - Q_0\mathbf{r}_0) + \sum_{T\in\mathcal{T}_h} h^{-1}\langle\mathbf{u}_0 - \mathbf{u}_b, Q_0\mathbf{r} - Q_b\mathbf{r}\rangle_{\partial T} \\
&\leq (\mathrm{osc}(\mathbf{f}, \mathcal{T}_h) + s^{1/2}(\mathbf{u}_h, \mathbf{u}_h))\|\nabla\mathbf{r}\| \\
&\leq (\mathrm{osc}(\mathbf{f}, \mathcal{T}_h) + s^{1/2}(\mathbf{u}_h, \mathbf{u}_h))\|\nabla\mathbf{u} - \nabla_w\mathbf{u}_h\|.
\end{aligned}$$

Then,

$$\begin{aligned}
(\nabla\mathbf{u} - \nabla_w\mathbf{u}_h, \mathbf{curl}\ \mathbf{s}) &= (\nabla\mathbf{u}, \mathbf{curl}\ \mathbf{s}) - (\nabla_w\mathbf{u}_h, \mathbf{curl}\ \mathbf{s}) = -(\nabla_w\mathbf{u}_h, \mathbf{Q}_h(\mathbf{curl}\ \mathbf{s})) \\
&= \sum_{T\in\mathcal{T}_h}\Big((\mathbf{u}_0, \nabla\cdot(\mathbf{Q}_h(\mathbf{curl}\ \mathbf{s})))_T - \langle\mathbf{u}_b, \mathbf{Q}_h(\mathbf{curl}\ \mathbf{s})\cdot\mathbf{n}\rangle_{\partial T}\Big) \\
&= \sum_{T\in\mathcal{T}_h}\Big(\langle\mathbf{u}_0 - \mathbf{u}_b, (\mathbf{Q}_h(\mathbf{curl}\ \mathbf{s}))\cdot\mathbf{n}\rangle_{\partial T} - (\mathbf{u}_0, \mathbf{curl}\ \mathbf{s})_T\Big) \\
&= \sum_{T\in\mathcal{T}_h}\Big(\langle\mathbf{u}_0 - \mathbf{u}_b, (\mathbf{Q}_h(\mathbf{curl}\ \mathbf{s}) - \mathbf{curl}\ \mathbf{s})\cdot\mathbf{n}\rangle_{\partial T}\Big).
\end{aligned}$$

By Cauchy-Schwarz inequality, the trace inequality and the inverse inequality, one obtains,

$$\langle\mathbf{u}_0 - \mathbf{u}_b, \mathbf{Q}_h(\mathbf{curl}\ \mathbf{s})\cdot\mathbf{n}\rangle_{\partial T} \leq C s_T^{1/2}(\mathbf{u}_h, \mathbf{u}_h)\|\mathbf{curl}\ \mathbf{s}\|_T.$$

The inverse inequality and the fact $\nabla\mathbf{curl}\ \mathbf{s} = 0$ imply

$$\begin{aligned}
\langle\mathbf{u}_0 - \mathbf{u}_b, \mathbf{curl}\ \mathbf{s}\cdot\mathbf{n}\rangle_{\partial T} &= \sum_{e\subset\partial T}\langle\mathbf{u}_0 - \mathbf{u}_b, \mathbf{curl}\ \mathbf{s}\cdot\mathbf{n}\rangle_e \\
&\leq \sum_{e\subset\partial T}\|\mathbf{u}_0 - \mathbf{u}_b\|_{H^{1/2}(e)}\|\mathbf{curl}\ \mathbf{s}\cdot\mathbf{n}\|_{H^{-1/2}(e)} \\
&\leq C\Big(\sum_{e\subset\partial T} h_T^{-1/2}\|\mathbf{u}_0 - \mathbf{u}_b\|_e^2\Big)^{1/2}\|\mathbf{curl}\ \mathbf{s}\|_{H(\mathrm{div},T)} \\
&\leq C s_T^{1/2}(\mathbf{u}_h, \mathbf{u}_h)\|\mathbf{curl}\ \mathbf{s}\|_T.
\end{aligned}$$

Combining the above estimates and taking summation over T gives

$$(\nabla \mathbf{u} - \nabla_w \mathbf{u}_h, \mathbf{curl}\ \mathbf{s}) \leq C s^{1/2}(\mathbf{u}_h, \mathbf{u}_h) \|\mathbf{curl}\ \mathbf{s}\|. \tag{4.8}$$

Besides,

$$\begin{aligned}(\nabla \mathbf{u} - \nabla_w \mathbf{u}_h, q\mathrm{I}) &= (\nabla \cdot \mathbf{u}, q) - (\nabla_w \mathbf{u}_h, \mathbb{Q}_h(q)\mathrm{I}) = -(\nabla_w \mathbf{u}_h, \mathbb{Q}_h(q)\mathrm{I}) \\ &= (\mathbf{u}_0, \nabla \mathbb{Q}_h(q)) - \sum_{T\in\mathcal{T}_h} \langle \mathbf{u}_b \cdot \mathbf{n}, \mathbb{Q}_h(q)\rangle_{\partial T} = \sum_{T\in\mathcal{T}_h} (\nabla_w \cdot \mathbf{u}_h, \mathbb{Q}_h(q))_T \\ &= 0.\end{aligned}$$

Using all the above estimates, we arrive at the conclusion. □

LEMMA 4.2. *Let $p \in L_0^2(\Omega)$ and $p_h \in W_h$ be the solutions of (1.1)-(1.3) and weak Galerkin scheme (2.3)-(2.4), respectively. Then there exists a positive constant C such that:*

$$\|p - p_h\| \leq C\eta. \tag{4.9}$$

Proof. For $\mathbf{v} \in H_0^1(\Omega)$, one has

$$\begin{aligned}(\nabla \cdot \mathbf{v}, p - p_h) &= -(\mathbf{f}, \mathbf{v}) + (\nabla \mathbf{u}, \nabla \mathbf{v}) - (\nabla \cdot \mathbf{v}, p_h) \\ &= -(\mathbf{f}, \mathbf{v}) + (\nabla \mathbf{u}, \nabla \mathbf{v}) - (\nabla_w \cdot Q_h \mathbf{v}, p_h) \\ &= (\mathbf{f}, Q_0\mathbf{v} - \mathbf{v}) + (\nabla \mathbf{u}, \nabla \mathbf{v}) - (\nabla_w \mathbf{u}_h, \nabla_w Q_h \mathbf{v}) - \sum_{T\in\mathcal{T}_h} h^{-1} \langle \mathbf{u}_0 - \mathbf{u}_b, Q_0\mathbf{v} - Q_b\mathbf{v}\rangle_{\partial T} \\ &= (\mathbf{f} - \mathbf{f}_h, Q_0\mathbf{v} - \mathbf{v}) + (\nabla \mathbf{u} - \nabla_w \mathbf{u}_h, \nabla \mathbf{v}) - s(\mathbf{u}_h, Q_h\mathbf{v}) \\ &\leq C\|\nabla \mathbf{v}\| \left(\mathrm{osc}(\mathbf{f}, \mathcal{T}_h) + \|\nabla \mathbf{u} - \nabla_w \mathbf{u}_h\| + s^{1/2}(\mathbf{u}_h, \mathbf{u}_h) \right) \\ &\leq C\|\nabla \mathbf{v}\|\, \eta.\end{aligned}$$

The inf-sup condition induces the following

$$\begin{aligned}\|p - p_h\| &\lesssim \sum_{\mathbf{v}\in[H_0^1(\Omega)]^2} \frac{(\nabla \cdot \mathbf{v}, p - p_h)}{\|\mathbf{v}\|_1} \\ &\leq C\eta,\end{aligned}$$

and thus completes the proof. □

THEOREM 4.3. *Let $\mathbf{u} \in H_0^1(\Omega)$, $p \in L_0^2(\Omega)$ and $\mathbf{u}_h \in V_h^0$, $p_h \in W_h$ be the solutions of (1.1)-(1.3) and weak Galerkin scheme (2.3)-(2.4), respectively. Then there exists a positive constant C such that:*

$$\|\mathbf{u} - \mathbf{u}_h\|_{1,h} + \|p - p_h\| \leq C\eta. \tag{4.10}$$

Proof. By combining Lemma 4.1 and Lemma 4.2, one can derive this theorem. □

Define

$$\|\mathbf{u} - \mathbf{u}_h\|_{1,T}^2 = \|\nabla \mathbf{u} - \nabla_w \mathbf{u}_h\|_T^2 + s_T(\mathbf{u}_h, \mathbf{u}_h).$$

Then we can obtain the following local lower bound automatically.

THEOREM 4.4. *The local estimator η_T is defined in (4.1). Then*

$$\eta_T^2 \leq \|\mathbf{u}-\mathbf{u}_h\|_{1,T}^2 + \|p-p_h\|_{0,T}^2 + osc^2(\mathbf{f},T). \tag{4.11}$$

5. Numerical Example. In this section, we shall validate the proposed algorithm with several tests. First, we shall explore the convergence properties of errors measured in $|||\cdot|||$-norm and $\|\cdot\|_{1,h}$-norm and the error estimator η. In the following, we shall measure

$$\text{Eng-Error: } |||Q_h\mathbf{u}-\mathbf{u}_h|||,$$

$$H^1\text{-Norm: } \|\mathbf{u}-\mathbf{u}_h\|_{1,h} = \left(\sum_{T\in\mathcal{T}_h} \|\nabla\mathbf{u}-\nabla_w\mathbf{u}_h\|_T^2 + h_T^{-1}\|\mathbf{u}_0-\mathbf{u}_b\|_{\partial T}^2\right)^{1/2},$$

$$L^2\text{-Norm: } \|p-p_h\| = \left(\sum_{T\in\mathcal{T}_h} \|p-p_h\|_T^2\right)^{1/2}.$$

Futhermore we denote

$$\|(\mathbf{u}-\mathbf{u}_h; p-p_h)\|_h := (|||Q_h\mathbf{u}-\mathbf{u}_h|||_{1,h}^2 + \|p-p_h\|^2)^{1/2}, \tag{5.1}$$

which will be denoted as H1error in Figure 5.2, 5.3, 5.9, and 5.10.

Two different types of effectivity for the estimator are defined as follows,

$$\text{Eff-1} = \frac{|||Q_h\mathbf{u}-\mathbf{u}_h|||}{\eta}, \tag{5.2}$$

$$\text{Eff-2} = \frac{\|(\mathbf{u}-\mathbf{u}_h; p-p_h)\|_h}{\eta}. \tag{5.3}$$

5.1. Example 1. Let domain $\Omega = (0,1)\times(0,1)$ and the exact solution be chosen as:

$$\mathbf{u} = \begin{pmatrix} -\exp(x)\big(y\cos(y)+\sin(y)\big) \\ \exp(x)y\sin(y) \end{pmatrix}, \ p = 2\exp(x)\sin(y). \tag{5.4}$$

The weak Galerkin scheme with $k=1,2,3$ has been used to solve Stokes equation. In this test, the exact solution is smooth and we can expect optimal rate in convergence. Table 5.1 reports the error profiles and convergence results. It can be observed that the errors measured in $|||\cdot|||$-norm and $\|\cdot\|_h$-norm converge at the order $\mathcal{O}(h^k)$, which agrees with the theoretical results. Also the effectivity index is close to a constant, thus validating our analytical predictions.

Next, we shall perform the adaptive finite element methods to solve singular problems. A typical adaptive algorithm are shown as follows:

$$\text{Solve} \rightarrow \text{Estimate} \rightarrow \text{Mark} \rightarrow \text{Refine}.$$

In our numerical experiments, the following steps shall be performed: we first solve weak Galerkin numerical solution on a given initial mesh, estimate the a posteriori

TABLE 5.1
Example 1. Error profiles and convergence results.

$1/h$	η	order	$\|\|\|\mathbf{u}_h - Q_h\mathbf{u}\|\|\|$	order	Eff-1	$\|(\mathbf{u}-\mathbf{u}_h; p-p_h)\|_h$	order	Eff-2
				$k=1$				
2	6.7814E-01		6.6829E-01		0.99	1.2240E+00		1.80
4	5.6302E-01	0.27	5.5775E-01	0.26	0.99	8.2631E-01	0.57	1.47
8	3.7976E-01	0.57	3.4907E-01	0.68	0.92	4.7498E-01	0.80	1.25
16	2.1590E-01	0.81	1.9113E-01	0.87	0.89	2.4438E-01	0.96	1.13
32	1.1344E-01	0.93	9.8875E-02	0.95	0.87	1.2201E-01	1.00	1.08
64	5.7739E-02	0.97	5.0032E-02	0.98	0.87	6.0710E-02	1.01	1.05
				$k=2$				
2	1.1093E-01		1.3203E-01		1.19	2.0762E-01		1.87
4	5.4268E-02	1.03	5.8601E-02	1.17	1.08	7.8419E-02	1.40	1.45
8	1.9410E-02	1.48	1.8833E-02	1.64	0.97	2.4817E-02	1.66	1.28
16	5.6318E-03	1.79	5.2363E-03	1.85	0.93	6.9264E-03	1.84	1.23
32	1.5042E-03	1.90	1.3746E-03	1.93	0.91	1.8243E-03	1.92	1.21
64	3.8813E-04	1.95	3.5187E-04	1.97	0.91	4.6786E-04	1.96	1.21
				$k=3$				
2	8.4639E-03		9.1513E-03		1.08	1.3916E-02		1.64
4	1.8507E-03	2.19	1.8674E-03	2.29	1.01	2.7447E-03	2.34	1.48
8	3.1269E-04	2.57	2.9126E-04	2.68	0.93	4.4243E-04	2.63	1.41
16	4.4535E-05	2.81	4.0109E-05	2.86	0.90	6.1946E-05	2.84	1.39
32	5.9606E-06	2.90	5.2462E-06	2.93	0.88	8.1996E-06	2.92	1.38
64	7.6508E-07	2.96	6.7257E-07	2.96	0.88	1.0834E-06	2.92	1.42

error estimator η_T and η, mark the elements that require further refinement, refine the marked elements, and then repeat until the maximum iteration number is reached or a stopping criterion is satisfied. The Dörfler/bulk marking method is used in the mark procedure.

The mesh is refined by two different methods (as [26]): quadrilateral refinement (refinement-1) or pentagonal refinement (refinement-2). The details of the mesh refinement can be found in reference [26]. Since our numerical scheme works on polygonal mesh, all the refinement will keep the local structure and does not need further refinement to remove hanging nodes.

5.2. Example 2. Let domain $\Omega = (0,1)\times(0,1)$ and the exact solution is chosen as:

$$\mathbf{u} = \begin{pmatrix} \frac{3}{2}\sqrt{r}(\cos(\frac{\theta}{2}) - \cos(\frac{3\theta}{2})) \\ \frac{3}{2}\sqrt{r}(3\sin(\frac{\theta}{2}) - \sin(\frac{3\theta}{2})) \end{pmatrix}, \ p = -6r^{-1/2}\cos(\frac{\theta}{2}). \tag{5.5}$$

It is known that this test problem has a corner singularity of order 0.5 at the origin $(0,0)$. Due to the singularity, the uniform grids can not produce the numerical scheme with optimal rate in convergence. The adaptive finite element methods can be applied to improve the numerical performance.

Figure 5.1 compares the two different refinement strategies for weak Galerkin element $k=3$ for chosen stopping criterion $\|(\mathbf{u}-\mathbf{u}_h; p-p_h)\|_h \le 0.05$. The H^1-error ($\|(\mathbf{u}-\mathbf{u}_h; p-p_h)\|_h$) and DOFs are shown as the caption. The refinements are focused on origin. It can be seen that the adaptive refinements guided by error estimator η_T accurately detect singularity in the problem.

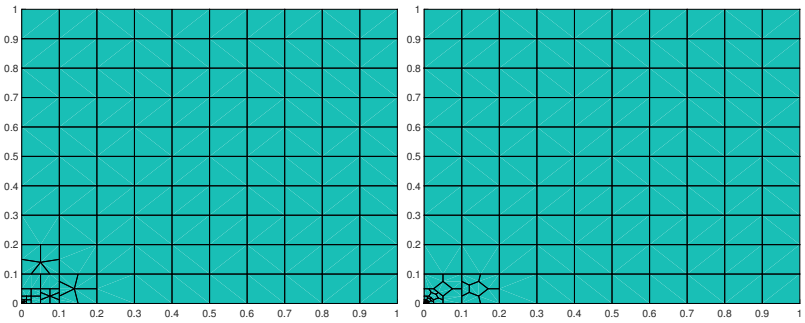

FIG. 5.1. *Example 2: Refined mesh by refinement-1 for* $\|(\mathbf{u}-\mathbf{u}_h; p-p_h)\|_h = 4.47E-02$ *and Dof*= 6090 *(Left); Refined mesh by refinement-2* $\|(\mathbf{u}-\mathbf{u}_h; p-p_h)\| = 4.55E-02$ *and Dof*=6560 *(Right).*

Figures 5.2-5.3 present the convergence results of $k = 1, 2, 3$ with two different refinement methods. Both of them show the optimal rates in convergence with respect to degrees of freedom, which are $\mathcal{O}(\text{Dof}^{-k/2})$.

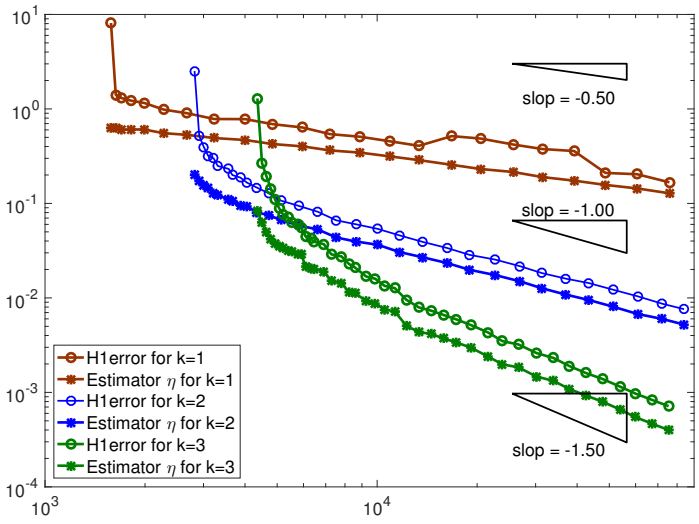

FIG. 5.2. *Example 2: Convergence results for refinement-1.*

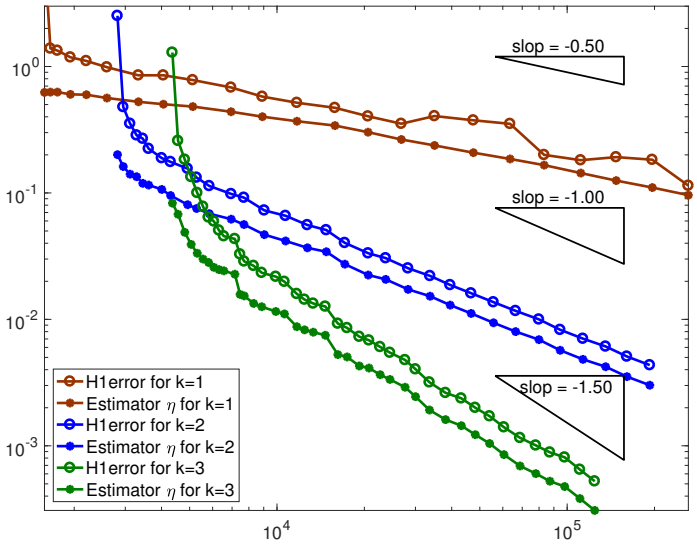

FIG. 5.3. *Example 2: Convergence results for refinement-2.*

Next, we start with an initial mesh which is a combination of mixed polygons shown as Figure 5.4. This mesh is generated by randomly moving the interior vertices from structured mesh. It is noted that this mesh contains non-convex polygons. The same adaptive weak Galerkin method will be performed: two different refinement strategies will be adopted for the marked cells. Figure 5.5 compares the two different refinement strategies for weak Galerkin element $k = 3$ with chosen stopping criterion $\|(\mathbf{u} - \mathbf{u}_h; p - p_h)\|_h \leq 0.05$. Again, the singularity at origin is captured by the refinement.

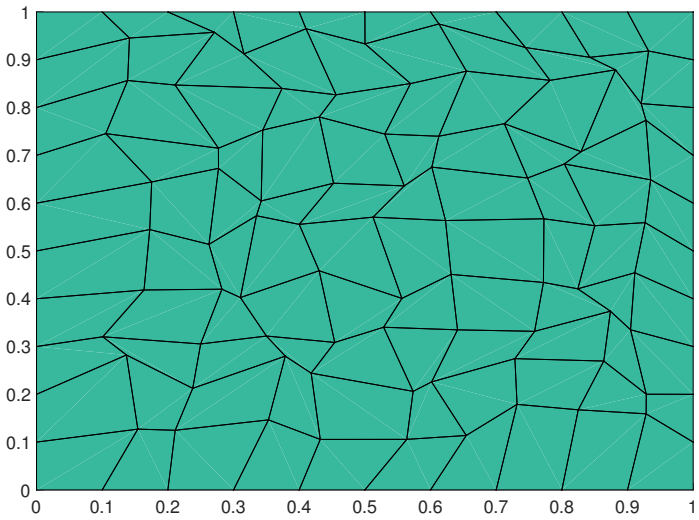

FIG. 5.4. *Example 2: Initial mesh with general polygons.*

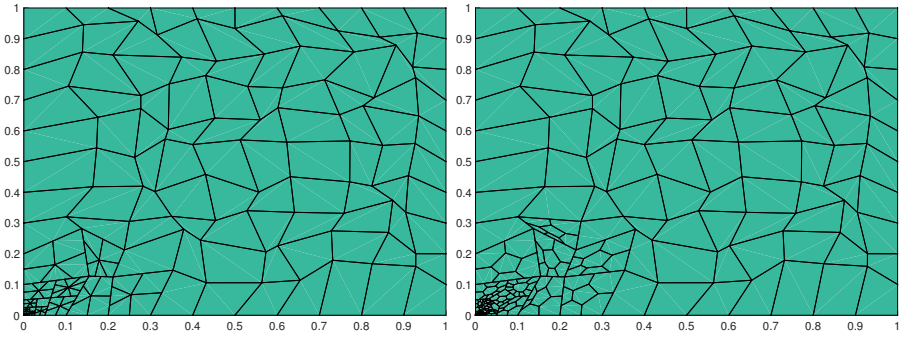

FIG. 5.5. *Example 2: Refined mesh by refinement-1 (Left); Refined mesh by refinement-2 (Right).*

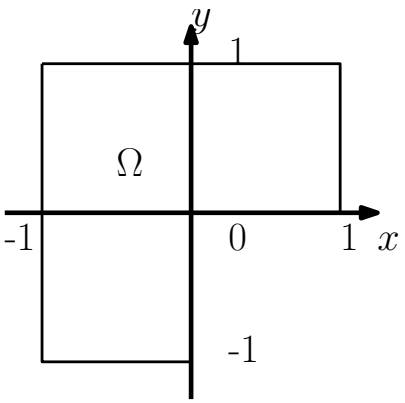

FIG. 5.6. *Example 3: Domain of L-shape problem.*

5.3. Example 3. L-shape problem: let domain $\Omega = (0,1)^2 \backslash [0,1] \times [-1,0]$ (as shown in Figure 5.6). The exact solution is chosen as follows

$$\mathbf{u} = r^{\lambda} \begin{pmatrix} (1+\lambda)\sin(\theta)\Phi(\theta) + \cos(\theta)\Phi_{\theta}(\theta) \\ \sin(\theta)\Phi_{\theta}(\theta) - (1+\lambda)\cos(\theta)\Phi(\theta) \end{pmatrix},$$

$$p = \frac{-r^{\lambda-1}((1+\lambda^2)\Phi_{\theta}(\theta) + \Phi_{\theta\theta\theta}(\theta))}{1-\lambda}, \tag{5.6}$$

with

$$\begin{aligned} \Phi(\theta) = & \frac{\sin((1+\lambda)\theta)\cos(\lambda\omega)}{1+\lambda} - \cos((1+\lambda)\theta) \\ & - \frac{\sin((1-\lambda)\theta)\cos(\lambda\omega)}{1-\lambda} + \cos((1-\lambda)\theta), \\ \omega = & \frac{3\pi}{2}, \\ \lambda = & 856399/1572864 \approx 0.54448. \end{aligned}$$

This solution satisfies the homogeneous Stokes equation. But $\mathbf{u} \notin [H^2(\Omega)]^2$ and $p \notin H^1(\Omega)$. Due to the singularity in the problem, we shall apply adaptive weak Galerkin algorithm to improve numerical performance in the computing.

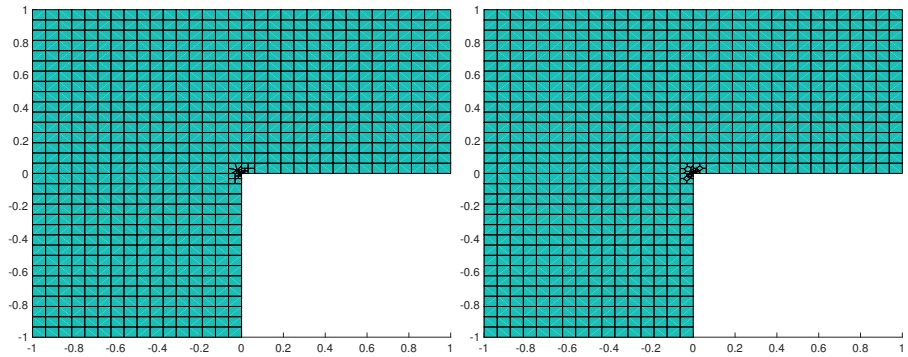

FIG. 5.7. *Example 3: Refined mesh by refinement-1 for* $\|(\mathbf{u}-\mathbf{u}_h; p-p_h)\|_h = 8.60E-02$ *and Dof*= 34792 *(Left); Refined mesh by refinement-2* $\|(\mathbf{u}-\mathbf{u}_h; p-p_h)\| = 9.50E-02$ *and Dof*=35618 *(Right).*

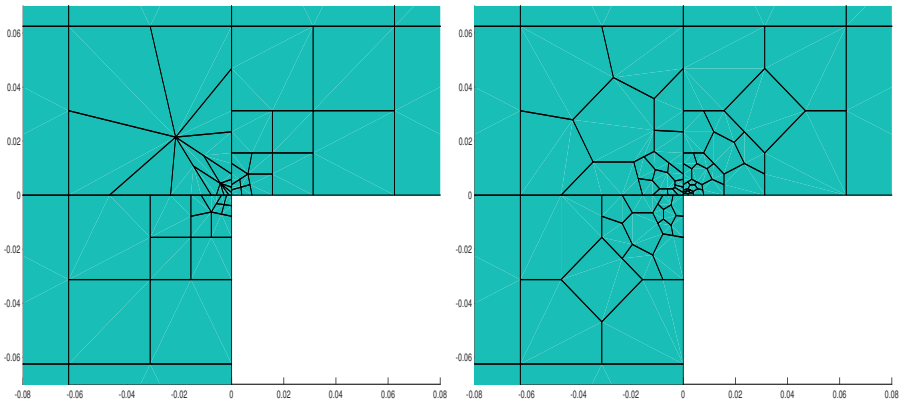

FIG. 5.8. *Example 3: Zoom in view for Fig.5.7 on* $[-0.08, 0.08] \times [-0.07, 0.07]$*: refinment-1 (Left); refinment-2 (right).*

Figure 5.7-5.8 compares two different refinement methods with $k = 3$ by setting stopping criteria as $\|(\mathbf{u}-\mathbf{u}_h; p-p_h)\|_h \leq 0.01$. Both methods perform the refinement centered at origin, and thus can capture singularity in the problem.

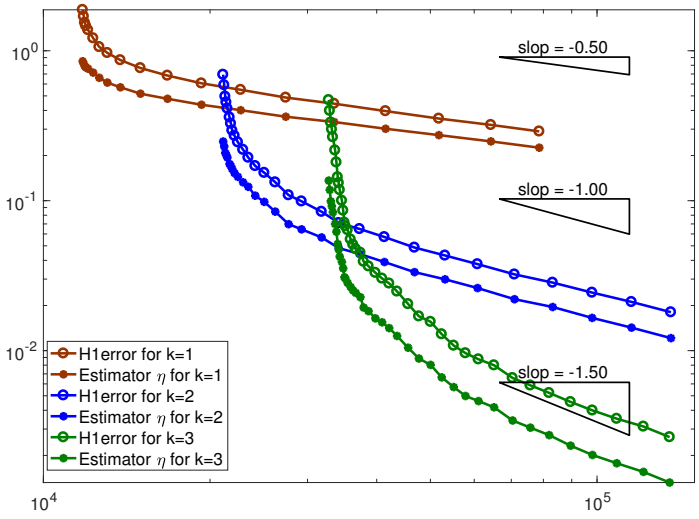

FIG. 5.9. *Example 3: Convergence results for refinement-1.*

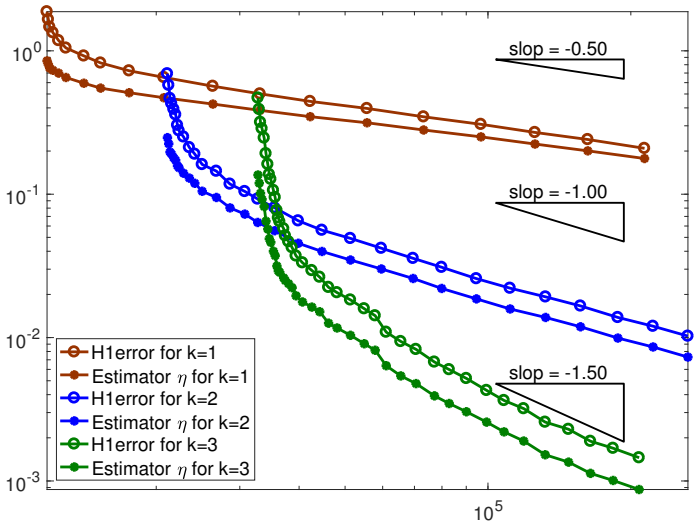

FIG. 5.10. *Example 3: Convergence results for refinement-2.*

Figures 5.9-5.10 report the convergence results for two different adaptive refinement methods. From both of them, one can observe the convergence rate with respect to DOFs is optimal at $\mathcal{O}(h^{-k/2})$. All the results confirm our theoretical conclusions.

5.4. Example 4. Driven cavity. Let $\Omega = (0,1)^2$ and the boundary condition for $\mathbf{u}$ be given as shown in Figure 5.11.

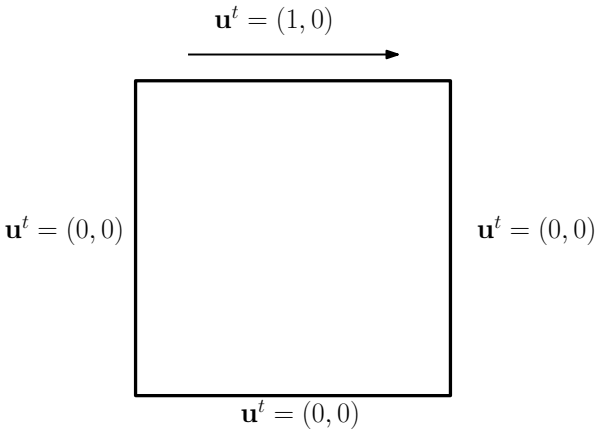

FIG. 5.11. *Example 4: Domain for driven cavity problem.*

Since the exact solution is not available, we only compare our refinement with results in previous literatures. As is known, the singularity are located at points $(0,1)$ and $(1,1)$. Thus we expect our adaptive refinement can locate these two points.

First we start with 10×10 uniform rectangular mesh. After 20 iterations with weak Galerkin finite element $k = 3$, the refinements as presented in Figure 5.12-5.13 focus on these two singularities as desired.

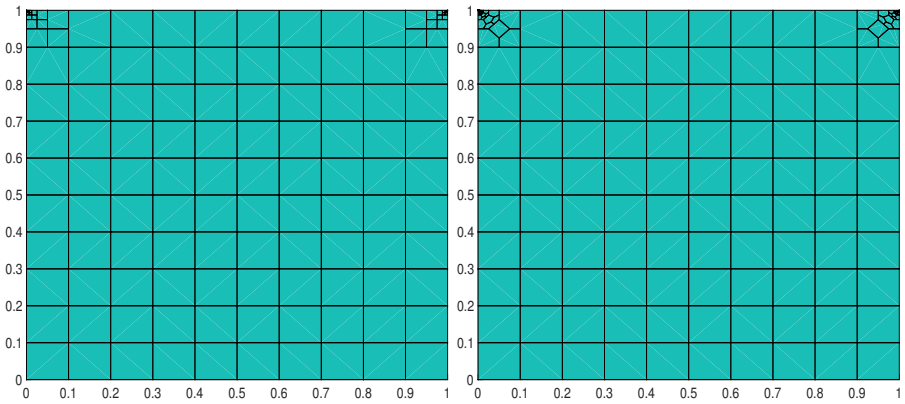

FIG. 5.12. *Example 4: Refined mesh by refinement-1 (left) and refinement -2 (right).*

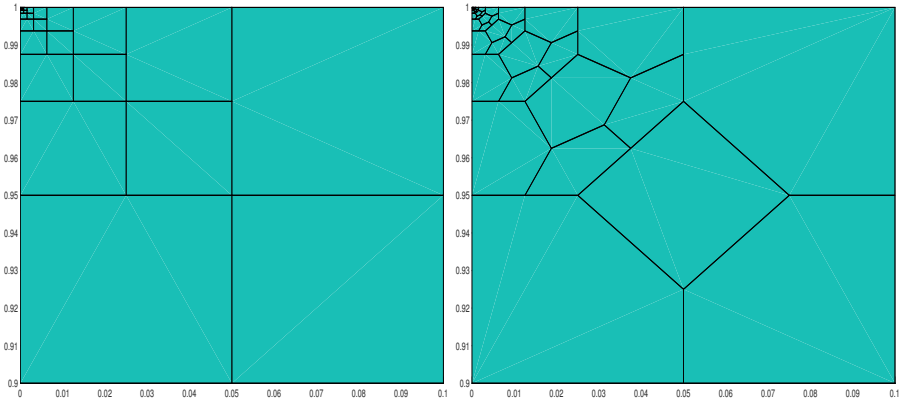

FIG. 5.13. *Example 4: Zoom in view for Fig.5.12 on* $[0, 0.1] \times [0.9, 1]$*: refinment-1 (Left); refinment-2 (right).*

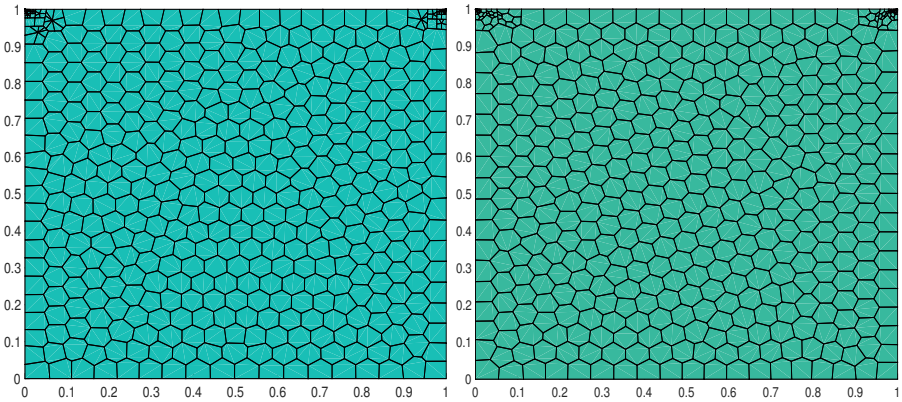

FIG. 5.14. *Example 4: Refined mesh by refinement-1 (left) and refinement-2 (right).*

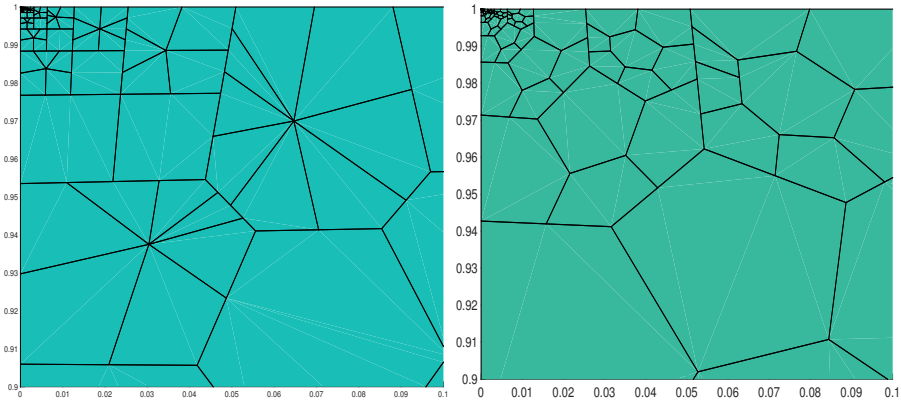

FIG. 5.15. *Example 4: Zoom in view for Fig.5.14 on* $[0, 0.1] \times [0.9, 1]$*: refinment-1 (Left); refinment-2 (right).*

Then we start with 20×20 uniform CVT mesh. After 20 iterations with weak

Galerkin finite element $k = 3$, the refinements are shown in Figure 5.14-5.15. Similar conclusions can be made for this test.

5.5. Example 5. Although our analysis is focused on the 2-dimensional Stokes equations, in this subsection, we shall perform our numerical scheme and compute the error estimators for the 3-dimensional (3D) Stokes problems. In this test, we shall take the domain as $\Omega = [0, 1]^3$ and the analytical solution for testing is chosen as follows:

$$\mathbf{u} = \begin{pmatrix} \sin z + \cos y \\ \sin x + \cos z \\ \sin y + \cos x \end{pmatrix}, \ p = x.$$

The weak Galerkin scheme with $k = 1$ ($\mathbf{u}_0 \in [P_1(T)]^3$, $\mathbf{u}_b \in [P_1(e)]^3$ and $p_h \in P_0(T)$) has been used to solve the 3D Stokes equations. We expect optimal rate in the convergence test in the global uniform refinement strategies.

The structured and unstructured tetrahedral meshes will be employed in this numerical experiment. The structured and unstructured initial meshes are shown in Figure 5.17-5.18. Then the global uniform refinement approach will be performed: one tetrahedron will be divided into eight smaller tetrahedrons (shown in Figure 5.16). The examples of first refinement (Level 2) can be found in Figure 5.17-5.18.

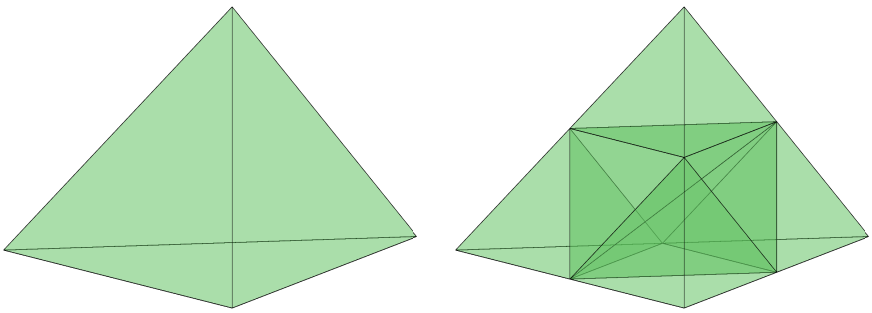

FIG. 5.16. *Example 5: one tetrahedron (left) and refinement (right).*

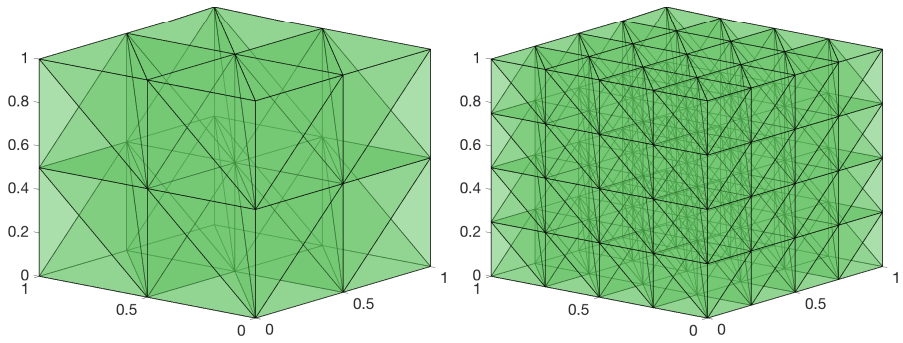

FIG. 5.17. *Example 5: Structured tetrahedral mesh: initial Mesh (left) and refinement (right).*

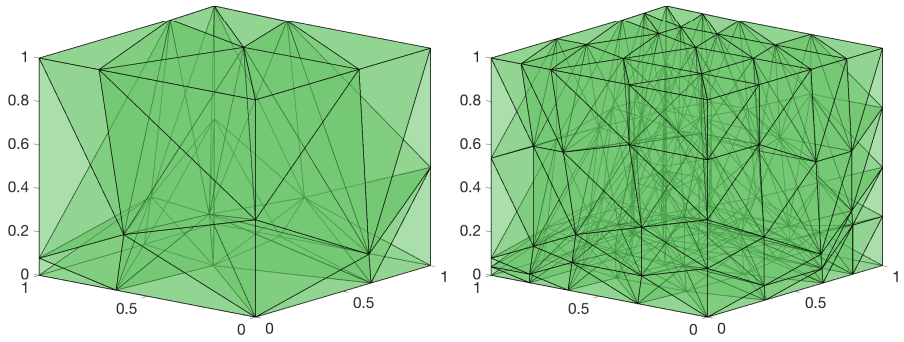

FIG. 5.18. *Example 5: Unstructured tetrahedral mesh: initial Mesh (left) and refinement (right).*

The error profiles and convergence results are presented in Table 5.2. It can be obtained from this table that the errors measured by $|||\mathbf{u}_h - Q_h\mathbf{u}|||$ and $\|(\mathbf{u}-\mathbf{u}_h; p-p_h)\|_h$ and error estimate η converge at the optimal rate of $\mathcal{O}(h)$, which agree with our expectations. Moreover, the effectivity index presented by Eff-1 and Eff-2 is close to a constant for both structured and unstructured meshes. Hence, all of the above tests validate our conclusions.

TABLE 5.2
Example 5. Error profiles and convergence results.

Lev	η	order	$\|\|\|\mathbf{u}_h - Q_h\mathbf{u}\|\|\|$	order	Eff-1	$\|(\mathbf{u}-\mathbf{u}_h; p-p_h)\|_h$	order	Eff-2
	Structured Mesh							
1	4.3751E-1		3.9591E-1		0.90	2.4187E-1		0.55
2	2.1856E-1	1.00	1.9970E-1	0.99	0.91	1.1213E-1	1.11	0.51
3	1.0923E-1	1.00	1.0025E-1	0.99	0.92	5.6148E-2	1.00	0.51
4	5.4611E-2	1.00	5.0337E-2	0.99	0.92	2.8144E-2	1.00	0.52
5	2.7314E-2	1.00	2.6179E-2	0.94	0.96	1.4114E-2	1.00	0.52
	Unstructured Mesh							
1	6.3593E-1		6.0010E-1		0.94	4.1294E-1		0.65
2	3.1860E-1	1.00	3.0363E-1	0.98	0.95	2.0265E-1	1.03	0.64
3	1.5937E-1	1.00	1.5254E-1	0.99	0.96	1.0179E-1	0.99	0.64
4	7.9685E-2	1.00	7.6270E-2	1.00	0.96	5.0897E-2	1.00	0.64
5	3.9843E-2	1.00	3.8135E-2	1.00	0.96	2.5449E-2	1.00	0.64

6. Conclusions and Future Work. In this paper, the simple a posteriori error estimate has been analyzed and applied to solve the Stokes equations. Theoretically, we proved the equivalence of the error estimator η and actual error measured in $\|\cdot\|_h$-norm. Numerically, several numerical experiments have been conducted to validate our theoretical conclusions. It shows that η is an efficient and reliable indicator to locate the singularity and thus guiding the local refinement for achieving optimal rate in convergence. Because our algorithm works on polygonal meshes, the refinement guided by indicator η_T will not propagate to the neighbor elements which do not need refinement.

In the future, our work will be extended to Stokes interface problems. The robust numerical schemes for high order approximation can be achieved by possibly combining our adaptive weak Galerkin algorithm with non-body fitted mesh. Because of

the fully computable property and the usage of polygonal meshes, our algorithm may motivate the designing of hp adaptive schemes. In the future, we shall investigate the numerical analysis and study the numerical performance for hp adaptive numerical schemes for solving elliptic equations. In addition, by preserving the local structure in the meshing, the savings in the adaptive approach for 3-dimensional problems would be more significant. However, the algorithm of efficient polyhedron type of refinement is still an open problem because of the geometry complexities. We will leave the investigation of the efficient and effective 3D polyhedron adaptive methods for the future research.

REFERENCES

[1] M. Ainsworth and J. Oden, A posteriori error estimation in finite element analysis, Pure Appl. Math., Wiley-Interscience, New York, 2000.

[2] M. Ainsworth and J. Oden, A unified approach to a posteriori error estimation using element residual methods, Numerische Mathematik, 65 (1993): 23-50.

[3] R. Bank and B. Welfert, A posteriori error estimates for the Stokes equations: a comparison, Computer Methods in Applied Mechanics and Engineering, 82 (1990): 323-340.

[4] R. Bank and B. Welfert, A posteriori error estimates for the Stokes problem, SIAM Journal on Numerical Analysis, 28 (1991): 591-623.

[5] R. Becker, M. Shipeng, and T. David, Adaptive nonconforming finite elements for the Stokes equations, SeMA Journal 50 (2010): 99-113.

[6] L. Beirão da Veiga, K. Lipnikov, and G. Manzini, Convergence analysis of the high-order mimetic finite difference method, Numer. Math., 113 (2009), 325-356.

[7] L. Beirão da Veiga, C. Lovadina, D. Mora, A Virtual Element Method for elastic and inelastic problems on polytope meshes, Comp. Meth. in Appl. Mech. and Eng.,1 (2015), 327-346.

[8] L. Beirão da Veiga, F. Brezzi, L. Marini and A. Russo, Mixed virtual element methods for general second order elliptic problems on polygonal meshes, ESAIM: M2AN, 50 (2016), 727-747.

[9] L. Beirão da Veiga, F. Brezzi, A. Cangiani, G. Manzini, D. Marini and A. Russo, Basic principles of virtual element methods, Math. Models Methods Appl. Sci., 23 (2013).

[10] L. Beirão da Veiga, F. Brezzi, D. Marini and A. Russo, Virtual Element Method for general second order elliptic problems on polygonal meshes, Math. Models Methods Appl. Sci., 26 (2016), 729-750.

[11] L. Beirão da Veiga, K. Lipnikov and G. Manzini, The mimetic finite difference method for elliptic problems, vol. 11 of MS&A. Modeling, Simulation and Applications. Springer, Cham, 2014.

[12] L. Beirão da Veiga and G. Manzini, A virtual element method with arbitrary regularity, IMA J. Numer. Anal., 34 (2014), 759-781.

[13] C. Bi and V. Cinting, A Posteriori Error Estimates of Discontinuous Galerkin Method for Nonmonotone Quasi-linear Elliptic Problems. J. of Sci. Comput., 55 (2013), 659-687.

[14] Z. Cai, X. Ye and S. Zhang, Discontinuous Galerkin finite element methods for interface problems: a priori and a posteriori error estimations, SIAM J. Numer. Anal., 49 (2011), 1761-1787.

[15] A. Cangiani, E. Georgoulis, T. Pryer and O. Sutton, A posteriori error estimates for the virtual element method, arXiv:1603.05855.

[16] L. Chen, J. Wang and X. Ye, a posteriori error estimates for Weak Galerkin finite element methods for second order elliptic problem, J. of Sci. Comp., 59 (2014), 496-511.

[17] B. Cockburn and K. Shi, Devising HDG methods for Stokes flow: An overview, Computers & Fluids 98 (2014), 221-229.

[18] E. Dari, D. Ricardo, and P. Claudio, Error estimators for nonconforming finite element approximations of the Stokes problem, Mathematics of computation, 64 (1995): 1017-1033.

[19] R. Duran, Mixed Finite Element Methods. Class Notes (2007).

[20] T. Gantumur, On the convergence theory of adaptive mixed finite element methods for the Stokes problem, arXiv:1403.0895.

[21] V. Gyrya1, K. Lipnikov1 and G. Manzini, The arbitrary order mixed mimetic finite difference method for the diffusion equation, ESAIM: M2AN, 50 (2016), 851-877.

[22] O. Karakashian and F. Pascal, A posteriori error estimates for a discontinuous Galerkinapproximation of second order elliptic problems, SIAM J. Numer. Anal., 45 (2003), 1777-1798.

[23] Y. Kondratyuk and R. Stevenson, An optimal adaptive finite element method for the Stokes problem, SIAM journal on numerical analysis, 46 (2008): 747-775.
[24] H. Li, L. Mu, X. Ye, A posteriori error estimates for the weak Galerkin finite element methods on polytopal meshes, preprint.
[25] C. Lovadina and D. Marini, A Posteriori Error Estimates for Discontinuous Galerkin Approximations of Second Order Elliptic Problems. J. of Sci. Comput., 40 (2009), 340-359.
[26] L. Mu. Weak Galerkin Based A Posteriori Error Estimates for Second Order Elliptic Interface Problems on Polygonal Meshes. Preprint.
[27] L. Mu, J. Wang and X. Ye, Weak Galerkin finite element methods on polytopal meshes, International Journal of Numerical Analysis and Modeling, 12 (2015): 31-53.
[28] L. Mu, J. Wang and X. Ye, Weak Galerkin finite element method for the Helmholtz equation with large wave number on polytopal meshes, IMA J. Numer. Anal., 35 (2015), 1228-1255.
[29] L. Mu, J. Wang, and X. Ye, A weak Galerkin finite element method for biharmonic equations on polytopal meshes, Numer. Meth. Partial Diff. Eq., 30 (2014), 1003-1029.
[30] L. Mu, J. Wang and X. Ye, Weak Galerkin finite element method for second-order elliptic problems on polytopal meshes, Int. J. of Numer. Anal. and Model., 12 (2015), 31-53.
[31] L. Mu, J. Wang, X. Ye and S. Zhang, A weak Galerkin finite element method for the Maxwell equations, J. of Sci. Comput., 65 (2015), 363-386.
[32] L. Mu, J. Wang, X. Ye and S. Zhao, A new weak Galerkin finite element method for elliptic interface problems, J. Comput. Phy., 325 (2016), 157-173.
[33] H. Houston, D. Schotzau, and T. Wihler, Energy norm shape a posteriori error estimation for mixed discontinuous Galerkin approximations of the Stokes problem, Journal of Scientific Computing, 22 (2005): 347-370.
[34] D.A. Di Pietro, E, Flauraud, M. Vohralik and S. Yousef, A posteriori error estimates, stopping criteria, and adaptivity for multiphase compositional Darcy flows in porous media, J. Comput. Phy., 276 (2014), 163-187.
[35] D.A. Di Pietro and A. Ern, Hybrid high-order methods for variable-diffusion problems on general meshes, Comptes Rendus Mathematique 353 (2015), 31-34.
[36] D.A. Di Pietro and A. Ern, A hybrid high-order locking-free method for linear elasticity on general meshes, Comput. Methods in Appl. Mech. and Engrg., 283 (2015), 1-21.
[37] D.A. Di Pietro, J. Droniou and A Ern, A discontinuous-skeletal method for advection-diffusion-reaction on general meshes, SIAM J. Numer. Anal., 53 (2015), 2135-2157.
[38] D.A. Di Pietro and A. Ern, Arbitrary-order mixed methods for heterogeneous anisotropic diffusion on general meshes, IMA J Numer Anal, 37 (2017), 40-63.
[39] D.A. Di Pietro and J. Droniou, A Hybrid High-Order method for Leray-Lions elliptic equations on general meshes, Math. Comp, 86 (2017): 2159-2191.
[40] W. Qiu and K. Shi, A superconvergent HDG method for the incompressible Navier-Stokes equations on general polyhedral meshes, IMA J. Numer, 36 (2016), 1943-1967.
[41] S. Rjasanow and W. Steffen, Higher order BEM-based FEM on polygonal meshes, SIAM Journal on Numerical Analysis 50 (2012): 2357-2378.
[42] C. Talischi, G. Paulino, A. Pereira and I. Menezes, PolyMesher: a general-purpose mesh generator for polygonal elements written in Matlab, Struct. Multidisc Optimiz., 45 (2012),309-328.
[43] R. Verfurth, A review of a posteriori error estimation and adaptive mesh-refinement techniques, Teubner Skripten zur Numerik. B.G. Willey-Teubner, Stuttgart, 1996.
[44] R. Verfurth, A posteriori error estimators for the Stokes equations, Numerische Mathematik, 55 (1989): 309-325.
[45] R. Verfurth, A posteriori error estimators for the Stokes equations II non-conforming discretizations, Numerische Mathematik, 60 (1991): 235-249.
[46] F. Wang, W. Han, J. Eichholze and X. Cheng, A posteriori error estimates for discontinuous Galerkin methods of obstacle problems. Nonlinear Analysis: Real World Applications, 22, (2015), 664-679.
[47] J. Wang, Y. Wang and X. Ye, unified a posteriori error estimator for finite element methods for the Stokes equations, Int. J. of Numer. Anal. and Model., 10 (2013), 551-570.
[48] J. Wang, X. Wang and X. Ye, finite element methods for the Navier-Stokes equations by H(div) elements, J. of Comput. Math., 26 (2008), 410-436.
[49] J. Wang, and X. Ye, A weak Galerkin finite element method for second-order elliptic problems, Journal of Computational and Applied Mathematics, 241 (2014), 103-115.
[50] J. Wang and X. Ye, A Weak Galerkin mixed finite element method for second-order elliptic problems, Math. Comp., 83 (2014), 2101-2126.
[51] J. Wang and X. Ye, A weak Galerkin finite element method for the Stokes equations, Adv. in Comput. Math., 42 (2016), 155-174.
[52] R. Wang, X. Wang, Q. Zhai, R. Zhang, A weak Galerkin finite element scheme for solving

the stationary Stokes equations, Journal of Computational and Applied Mathematics, 302 (2016): 171-185.

[53] S. Weier, Residual based error estimate and quasi-interpolation on polygonal meshes for high order BEM-based FEM, Computers & Mathematics with Applications, 73 (2017): 187-202.